International Journal of Scientific Research and Engineering Development-– Volume 4 Issue 5, Sep- Oct 2021

Available at www.ijsred.com

RESEARCH ARTICLE OPEN ACCESS

Modeling of a Cantilever-type Retaining Wall

Kempena Adolphe*, Mbilou Gampio Urbain**, Mbani Aspy Bronoski***, Boudzoumou Florent****, Rafael Guardado Lacaba*****

*Department of Geology, Faculty of Sciences and Technics, Marien Ngouabi University, Brazzaville-Congo
Email: akempena@gmail.com

**Department of Geology, Faculty of Sciences and Technics, Marien Ngouabi University, Brazzaville-Congo
Email : Muga68@yahoo.fr

***Department of Geology, Faculty of Sciences and Technics, Marien Ngouabi University, Brazzaville-Congo
Email: aspybronoskimbani@gmail.com

****Department of Geology, Faculty of Sciences and Technics, Marien Ngouabi University, Brazzaville-Congo
Email: boudzoumouf@gmail.com

***** Department of Geology, Faculty of Mines and Geology, Higher Institute of Mines and Metallurgy, Moa-CUBA
Email: rafaelguardado2008@gmail.com

--************************----------------------------------

ABSTRACT

The methods for dimensioning retaining walls are currently based on various calculation rules. Numerical methods have the advantage of taking into account more precisely the behavior of the soil and the soil-wall interface. In this research we studied the behavior of the concrete wall under the effect of head loading, which is considered to be one of the most important researches in the field of geotechnical engineering. This work is concerned with the numerical modeling of a retaining wall loaded at the head and a study of the influence of various parameters on the bearing capacity of the foundation and the stability of the retaining structure. This modeling was carried out using the finite element method. The results obtained are discussed and compared with those available in the literature. A good agreement of the results deduced from these approaches was noted.

Keywords: Retaining wall, load, foundation, finite element, Mohr-coulomb.

--************************----------------------------------

I. INTRODUCTION

Soil massifs stabilization is generally made by retaining structures construction. The interactions analysis between retaining structures and soil is the greatest concern in geotechnical engineering, especially in urban areas during the construction of complex structures near existing buildings or excavation work near buildings [1]. The stabilization of soil massifs is generally made by the construction of retaining structures [2,3]. This problem is currently one of the major concerns of engineers responsible for structures design. The development of computers and numerical methods has made it possible to simultaneously study walls behavior and supported soil masses, taking into account their deformations. Numerical methods allow the most complex geotechnical problems to be solved, providing information on deformations and displacements during construction and even after completion of the structure. These methods consist in solving partial differential equations; there are several techniques such as finite difference methods, finite volumes, spectral methods and the finite element method [4]. The aim of this work is therefore to study the stability of a retaining wall subjected to head loading from modeling techniques by the finite element method.

II. MATERIALS AND METHODS

A. *Digital model design*

As part of a modeling and analysis study of the behavior of a retaining wall in the presence of a loaded head, we carried out multiple simulations. The geometric dimensions chosen for the design of the digital model are those recommended for the modeling of a retaining wall in plane strain with the maximum sizes [5]. The soil and the structure are modeled by the Mohr-Coulomb constitutive law. A refined mesh was used to ensure the reproducibility and convergence of the results. The boundary conditions applied are managed automatically according to the default option. The calculations are performed by construction phase as the simulated case. It should be noted that different soil cohesion values were considered in the simulations conditioned by the reducing coefficient of soil-structure interaction noted Rinter.

B. *Mohr-coulomb model (MC model)*

The Mohr-Coulomb elastoplastic model used in this study includes five input parameters: E and υ for soil elasticity, c and φ for soil plasticity and ψ for soil dilatancy. This model represents a "first order" approximation to simulate the behavior of soils. Moreover, the initial soil conditions play an important role in almost all soil deformation problems. The value of k_0 is used to generate the initial horizontal soil stresses. Plasticity is associated with the development of irreversible deformations. In order to assess if it occurs or not in the calculations of a plasticity state, so a function of elastic limit f is introduced.

- **Perfectly plastic elastic behavior**

The soil real stress-strain behavior of is often characterized by an initial linear part, a peak or a breaking stress, then the soil softens to the residual stress. In a limit analysis, we must neglect the aspect of anti-hardening and consider the behavior of the soil having two straight lines (the dotted line). This soil which exhibits this property of continuous plastic flow is called a perfectly plastic soil.

- **Coulomb criterion and flow area**

It is important to know the soil behavior in a state of complex stress [6]. A flow criterion is the condition which characterizes the change of the soil from the elastic state to the plastic flow state with a complex stress state. In general, at any point and plane in a mass of soil, plastic flow occurs when the shear stress reaches a maximum value linearly proportional to the cohesion c and the normal stress σ_n.

$\tau = c + \sigma n \tan \phi$

- **Formulation of the Mohr-Coulomb model**

Here we present the formulation of the Mohr-Coulomb criterion. The Mohr-Coulomb full elastic limit condition comprises six functions of the elastic limit on the plane of the principal stresses (equation 1 to equation 6).

$$\int 1a = \frac{1}{2}(\sigma'_2 - \sigma'_3) + \frac{1}{2}(\sigma'_2 + \sigma'_3)\sin\phi - c\cos\phi \leq 0 \quad (1)$$

$$\int 1b = \frac{1}{2}(\sigma'_3 - \sigma'_2) + \frac{1}{2}(\sigma'_3 + \sigma'_2)\sin\phi - c\cos\phi \leq 0 \quad (2)$$

$$\int 2a = \frac{1}{2}(\sigma'_3 - \sigma'_1) + \frac{1}{2}(\sigma'_3 + \sigma'_1)\sin\phi - c\cos\phi \leq 0 \quad (3)$$

$$\int 2b = \frac{1}{2}(\sigma'_1 - \sigma'_3) + \frac{1}{2}(\sigma'_1 + \sigma'_3)\sin\phi - c\cos\phi \leq 0 \quad (4)$$

$$\int 3a = \frac{1}{2}(\sigma'_1 - \sigma'_2) + \frac{1}{2}(\sigma'_1 + \sigma'_2)\sin\phi - c\cos\phi \leq 0 \quad (5)$$

$$\int 3b = \frac{1}{2}(\sigma'_2 - \sigma'_1) + \frac{1}{2}(\sigma'_2 + \sigma'_1)\sin\phi - c\cos\phi \leq 0 \quad (6)$$

The two parameters representing the plastic model are the shear parameters c and φ. The elastic limit functions represent a hexagonal cone, as noted in the principal stress space where c = 0. In addition to the elastic limit functions, six plastic potential functions have been defined in this model.

$$g_{1a} = \frac{1}{2}(\sigma 2 - \sigma 3) + \frac{1}{2}(\sigma 2 + \sigma 3)\sin\psi \quad (7)$$

$$g_{1b} = \frac{1}{2}(\sigma'_3 - \sigma'_2) + \frac{1}{2}(\sigma'_3 + \sigma'_2)\sin\psi \quad (8)$$

$$g_{2a} = \frac{1}{2}(\sigma'_3 - \sigma'_1) + \frac{1}{2}(\sigma'_3 + \sigma'_1)\sin\psi \quad (9)$$

$$g_{2b} = \frac{1}{2}(\sigma'_1 - \sigma'_3) + \frac{1}{2}(\sigma'_1 + \sigma'_3)\sin\psi \quad (10)$$

$g_{3a} = \frac{1}{2}(\sigma'_1 - \sigma'_2) + \frac{1}{2}(\sigma'_1 + \sigma'_2)\sin\psi$ (11)

$g_{3b} = \frac{1}{2}(\sigma'_2 - \sigma'_1) + \frac{1}{2}(\sigma'_2 + \sigma'_1)\sin\psi$ (12)

Or ψ denotes the dilatancy angle of the soil.

- **Plate element**

The plate element allows the modeling of thin structures in contact or within the mass of the soil having considerable bending stiffness and normal (axial) stiffness. The plate element was used in this study to model the wall concrete. The properties required to define this element are the bending stiffness expressed by EI and the axial stiffness expressed by EA. Of these two values, an equivalent wall thickness d_{eq} is automatically calculated according to the following formula:

$$d_{eq} = \sqrt{12\frac{EI}{EA}}$$

Where E is the modulus of elasticity (Young's modulus) of the material constituting the plate, A is the cross section of the element and I is the section inertia moment. EI represents bending stiffness and EA represents axial stiffness. The plate element is discretized by a linear finite element with three degrees of freedom by node (joint): two degrees of freedom of translation (u_x and u_y) and only one degree of freedom of rotation (ϕz) in the x-y plane. When the one 6-node finite ground element is used, each plate element is defined by three nodes, whereas if the 15-node element is used, the 5-node plate element.

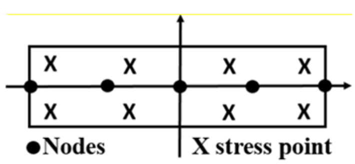

Fig. 1 Position of nodes and stress points in a 3-node and 5-node plate element [7].

The plate member is based on beam theory which allows beam deflection due to shear stress and bending. Furthermore, the length of the element can be changed if an axial force is applied. To determine whether the element reaches a state of plasticization or not, two maximum values for bending moment and axial force are prescribed. The bending moment and the axial force are evaluated from the stress at the stress points. The Gaussian stress points are shown in figure 1; where 3 node elements have two pairs of stress points and the 5 node elements have four pairs.

- **Interface elements**

An elastoplastic model makes it possible to describe the behavior of interfaces in the modeling of soil-structure interactions. Coulomb's criterion is used to distinguish the elastic behavior (where small displacements can appear at the interfaces) and the plastic behavior for which permanent slips can occur. To present the interface between the floor and the wall, elements of the interface are used. The connection of interface elements to ground elements is shown in figure 3.8. For a soil element having 15 nodes, the interface element has 10 nodes (five pairs). In this figure, one notices that the element of the interface has a thickness which does not exist in the formulation , the coordinates of each pair are identical (the thickness = 0).

Each interface has a virtual thickness which is an imaginary dimension used to define the properties of the interface material. The virtual thickness is calculated as the factor of the virtual thickness, a value of 0.1 is assumed by default, multiplied by the average dimension of the element. The average size is determined by the overall size of the mesh. The model used to simulate the behavior of the interface is an elastoplastic model. The Coulomb criterion is used to distinguish between elastic behavior and plastic behavior, in other words, this criterion is used to make difference between the small displacements which occur at the interface and the permanent sliding which can occur at the interface. So that the interface remains in the elastic domain, the shear stress is given by equation 13, whereas for the plastic behavior, the shear stress is presented by as so:

$|\tau| = c_i + \sigma_n \tan\phi_i$ (13)

c_i and ϕ are respectively the cohesion and friction angle of the interface. The properties of the interface are related to the properties of the soil resistance by a parameter called the resistance reduction factor for the Rinter interface; the properties of the interface are calculated using equations 14 and 15.

$c_i = R_{inter} x c_{sol}$(14)

$\tan \phi_i = R_{inter} x \tan \phi_{sol}$(15)

In general, for real interactions between soil and structure, the interface is weaker and more deformable than the associated soil layer, which means that the value of R_{inter} is less than 1. Values representative of R_{inter} in the case of interactions between different types of soils and structures can be found in the literature. In the absence of more detailed information, it is usual to take an approximate value R_{inter} = 2/3 for a sand-steel contact, and R_{inter} = 1/2 for a clay-steel contact; interactions with concrete give slightly higher values. Rinter values >1 should not normally be used.

C. Modeling and parametric study of the cantilever type wall

The work focuses on the numerical modeling and analysis of the behavior of a retaining cantilever wall, then loaded with a pavement at the head by the finite element method. We will study the stability of a cantilever wall supporting a soil mass with a horizontal surface supporting a rigid pavement subjected to a centered load. This study also examines the interaction between the wall and the soil. As well as the foundation soil with different characteristics to those of the embankment. After a series of numerical analyzes carried out on the adopted model of 6.1 m in total height and 10 m in width, with a wall height equal to 5 m, the width at the base is 2.8 m and its width at summit equal to 0.2 m. (figure 3).

D. Digital model geometry

The model considered for numerical simulations, calculations and behavioral study is represented in the figure below.

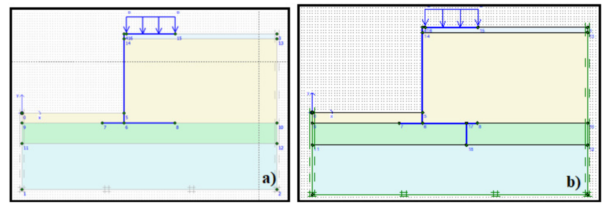

Fig. 2 Model geometry: a) wall without spade; b) wall with spade

- **Model geometry**

The problem does not present symmetry for this reason the modeling will be carried out for the totality of the plane geometrical model (2D) with 10 m of width and 6.1 m of height. The soil is mainly composed of three layers as a embankment layer at surface with 2.5 m of thick, an untreated gravel layer (GNT) with 0.8 m of thick and a second foundation layer having 1.8 m of considered depth. This massif is overloaded at the head by a rolling layer and a whole layer from crushing (TVC) with 0.2m of the thickness.

- **Model and parameters**

The Mohr-Coulomb model is the model used in our study; it requires to determine five parameters. The first two are E and υ (elasticity parameters). The other two are c and ϕ, the cohesion and the friction angle, respectively. These classic geotechnical parameters have been provided by the laboratory tests and are necessary for strain or stability calculations. The last parameter is the angle of "dilatancy" noted ψ; this is the least common setting. It can however be easily evaluated as $\psi = \phi - 30°$ for $\phi > 30°$, $\psi = 0°$ for $\phi < 30°$. The soil properties are shown in table 1.

E. Material characteristics

- **Properties of soil layers and interfaces**

The soil consists of a layer of silty sand wich the behavior model is the Mhor-Coulomb (MC). The parameters E_{ref}, c_{ref}, ψ and R_{inter} are variable depending on the simulated case as indicated in table 1.

TABLE I Soil characteristics.

Paramters	Symbol	Soil (silty sand)	Embankment	unit
Model of material	model	elastic perfectly plastic	elastic perfectly plastic	-
Type of behaviour	type	drained	drained	-
Soil density	γ_{hsoil}	17	20	[kn/m²]
Cohesion	c	31	1	[kn/m²]
Internal friction angle	ϕ	36	30	[°]
Angle of dilatancy	ψ	2/3 ϕ	_	[°]

- **Structural elements Characteristics**

In this model, the wall is made of concrete, assumed to be linear elastic (table 2).

TABLE II Wall characteristics

Parameters	Name	Value	Unit
Behavior type	material type	elastic	
Normal stiffness	EA	8.486e+06	kN/m
Bending stiffness	EI	1.514e+05	Kn/m^2
Equivalent thickness	d	0,463	m
Weight	w	62.065	kN/m
Poisson coefficient	υ	0,20	

Table III Concrete characteristics

Concrete density (kn / m3)	$\Gamma_{concrete}$= 24
Class C25/30 (Mn/m^2)	f_{c28} = 25
young's modulus (Mn/m^2)	E = 32164.2

These characteristics are provided by the National Laboratory of Habitat and Construction (L.N.H.C) of Djelfa (Brazzaville, Congo, 2020).

F. Validation of the digital model

In order to validate the numerical model, the total force exerted on the wall was determined using the analytical method:

- **Boundary conditions**

The boundary conditions are taken into account by blocking the horizontal and vertical displacements of the model using the default option (standard fixists). These boundary conditions are generated according to the following rules: the lower horizontal limit comprises the horizontal and vertical blockings ($u_x = u_y = 0$); as well as the vertical limit admits only the horizontal blockings ($u_x = 0$). The model of perfectly plastic elastic behavior is used by adopting the Mohr-Coulomb criterion. The mesh in the area near the wall is refined in order to obtain more reliable results. The model is discretized using triangles at 15 nodes. The base of the sole is considered perfectly rough. A local refinement of the mesh was carried out in the areas of strong stress gradients, that is to say in the vicinity and under its base (Figure 4).

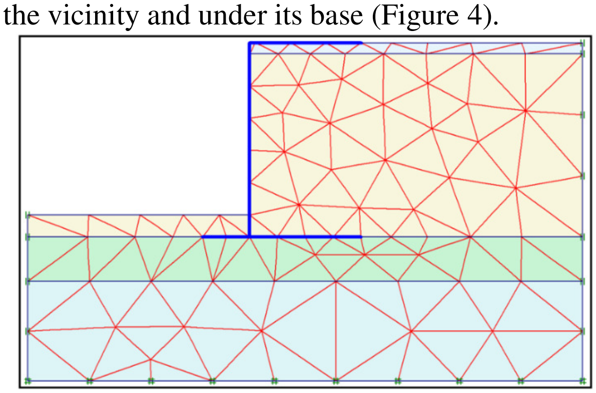

Fig. 4 Mesh model

- **Initial conditions**

The initial conditions require generating initial stresses. Initial stresses were then generated by taking the value of k_o automatically proposed according to Jaky's formula [8]. Then we kept the weight of the soil at 1, which corresponds to a total application of gravity. K_o = 1-sinφ (Jaky's formula) (figure 5).

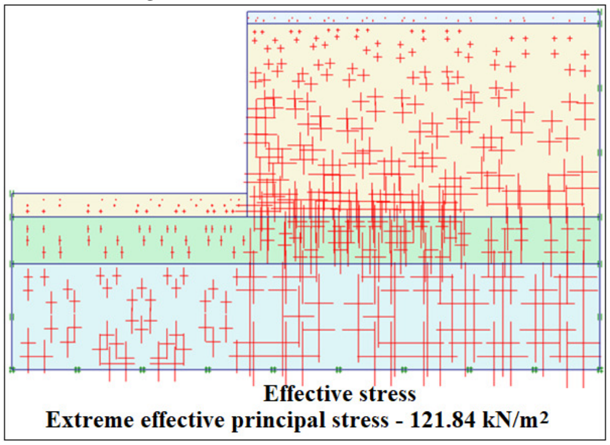

Fig. 5 Initial stresses generation

III. RESULTS

G. *Modeling and parametric study*

- **Total displacement (Figure 6)**

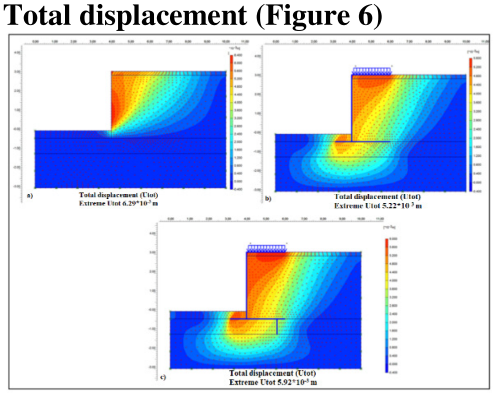

Fig. 6 Maximum total displacement

Figure 6 represents a comparison between the total displacements evolution. We appreciate that the wall reduces displacements in the case of unreinforced soil ($6.29*10^{-3}$m) that is more than reinforced soil ($5.22*10^{-3}$ mm) and $5.92*10^{-3}$ m.

a) Unreinforced soil (without wall): the maximum total displacement is $6.29*10^{-3}$ m.

I. Reinforced soil

- Soil with wall without spade + road: the maximum total displacement is $5.22*10^{-3}$ m.
- Soil with wall + spade + road: the maximum total displacement is $5.92*10^{-3}$ m.

K. *Horizontal displacement*

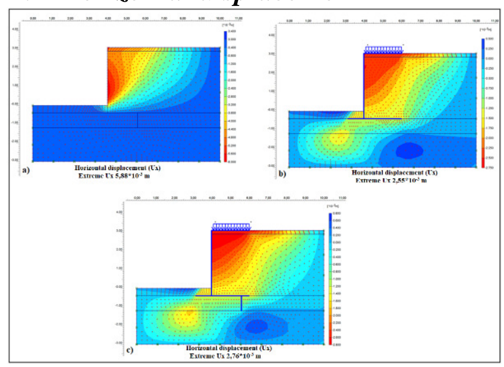

Fig. 7 Horizontal displacement

The figure 7 shows the comparison between horizontal displacements evolutions where we observe that in the case of a wall with a spade the horizontal displacements are reduced. That is to say the spade stops the horizontal stresses evolution. In fact we appreciate a low horizontal displacement value in the case of a wall with a spade. So we have :

- An horizontal displacement of $5,88*10^{-3}$ m for unreinforced soil and without load
- An horizontal displacement of -$2,55*10^{-3}$ m for reinforced soil with wall and without spade and load at the head.
- An horizontal displacement of -2.76*10-3 m m for reinforced soil with wall and with spade and lod at the head.

L. Vertical displacement

In figure 8 we observe a comparison between vertical displacements evolution. the maximum vertical displacement representing the maximum settlement is -0.00464m that testifies to the punching stability of the structure, even if a slight increase in the vertical stress is observed in the case of a wall with a spade of -0.00539 m, this is due to the fact that the presence of the spade prevents lateral displacements, but to a lesser extent favors vertical displacement, even if this settlement can be considered less important compared to the observed value. It is obvious that the distribution of vertical stresses is regular in the massif far from the wall, this distribution is triangular according to equation $\sigma = \gamma.z$, moreover this distribution is almost regular in the vicinity of the wall and under the foundation as shown by the isovalues in the figure above. The Figure 8 also shows that the vertical stresses are very important under the left and right ends of the base of the wall which prevents significant settlement below level and retains the wall rotation around its ends.

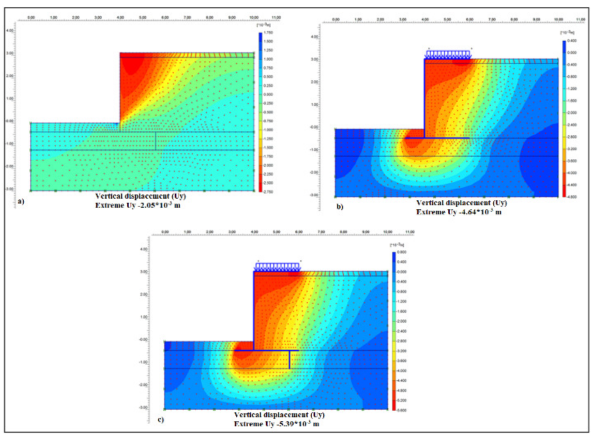

Fig. 8 Vertical displacement

IV. DISCUSSION

This paper presents a parametric study aimed at identifying the influence of certain parameters on the results of numerical simulations concerning a retaining wall loaded at the head by a rolling layer. By studying the influence of each geometric parameter separately we get a reasonable study of this wall. The geometric parameters taken into consideration include a wall without a spade and with a spade. For this purpose, the influence of the spade on the resistance to sliding and tilting of the wall is obvious. In both cases the distribution of total incremental displacement for the case of a wall without spade the displacements are greater compared to the wall with spade, this difference between the displacements is due to the thrust developed behind the wall without spade, of which the horizontal stresses increase in power which is the opposite for the case of a wall with a spade. This aspect explains the deference between the displacement illustrated in the two situations a and b presented in Figure 7. The results obtained are in agreement with literatures [9, 10, 4, 7].

V. CONCLUSION

This study allowed us to bring together a great deal of knowledge on retaining structures, their behavior and the different design approaches under the loading action. The numerical simulations that were implemented are used to analyze the influence of each parameter on the behavior of a retaining structure loaded at the head. The development of the digital model is based on a previous study which allowed us to validate before carrying out the parametric study. Also the results obtained are very satisfactory as appreciated on displacement maps which are similar to those published in the literature. The parametric analysis is of particular interest because it makes it possible to assess parameters influence on model reliability results.

VI. REFERENCES

[1] G.A.Fenton, Griffiths D.V., Williams, M.B..*reliability of traditional retaining wall design. géotechnique*, 2005, 55(1), 55–62.

[2] N.Magoura,comportement d'un écran de soutènement renforcé par des armatures métalliques. mémoire de magister. université de m'sila, 2017.

[3] K. Terzaghi, Theoretical soil mechanics. New york, wiley.

[4] P. Mestat (1998). état de contraintes initiales dans les sols et calcul par éléments finis.

(bulletin des laboratoires des ponts et chaussées, 215, p. 15-32, 1943.

[5] C.William, Acknowledgement, and Part1: Geometry space, boundaries and meshing – Part2: Initial stresses and Phi-c reduction, 2008, Plaxis seminar-Vietnam.

[6] R. Lancellotta, analytical solution of passive earth pressure. Géotechnique, 52, no. 8, 617–619, 2002.

[7] P. Mestat, Lois de comportement des géomatériaux et modélisation par la méthode des éléments finis. laboratoire central des ponts et chaussées, erlpc, série géotechnique, gt 52, p194, 1993.

[8] J. Jaky, the coefficient of earth pressure at rest. in hungarian a nyugalmi nyomas tenyezoje. J. Soc. Hung. Eng. Arch. (magyar mernok es epitesz-egylet kozlonye), 355– 358, 1944.

[9] K. Georgiadis, The influence of load inclination on the undrained bearing capacity of strip footings on slopes. computers and geotechnics, 37(3), 311-322, 2010.

[10] J. G. Maloum, S., & Sieffert, Interaction sol-fondation superficielle au voisinage de la crête d'un talus : analyse de la capacité portante. revue française de géotechnique, 100, 83-89, 2002.